Sustainable Chemical Engineering
https://ojs.wiserpub.com/index.php/SCE/

UNIVERSAL WISER PUBLISHER

Research Article

Direct Photocatalytic CO_2 Reduction in Rich Amine for Formic Acid Production

Syafiqa Mohd Saleh[1,2*], Oh Pei Ching[2], M Zulfan Naim Zulkifli[1], Tai Xin Hong[1], Masniroszaime M Zain[1], Thiam Leng Chew[2]

[1]Petronas Research Sdn. Bhd., Off Jalan Ayer Itam, Bangi Institutional Area, Kajang, Selangor, 43000, Malaysia
[2]CO_2 Research Centre (CO_2RES), Department of Chemical Engineering, Universiti Teknologi PETRONS, Tronoh, Perak, 32610, Malaysia
E-mail: syafiqa_saleh@petronas.com

Received: 15 September 2025; **Revised:** 29 December 2025; **Accepted:** 9 January 2026

Abstract: Direct CO_2 reduction from rich amine is advantageous as this allows for a push a step closer to realising the concept of integrated carbon capture and utilization. This study looks into the application of using a photocatalytic process to convert the absorbed CO_2 into formic acid. A slurry system using TiO_2 as a photocatalyst was used together with a Ultraviolet C (UVC) light source and based on Response Surface Methodology (RSM) analysis, with the empirical model R^2 of 0.9080 achieved, the optimum yield of formic acid obtained was 108 μmol/g cat·hr when running with 0.2 g TiO_2, at 50 °C and a 3-hour operation. The yield of product obtained is comparable to others reported in the literature. A moderate kinetic model fit was achieved for formic acid production with an R^2 of 0.64 and Root Mean Squared Deviation (RMSD) of 14.08. Comparison is done between slurry and immobilised TiO_2 where a 33% drop in yield was achieved when the photocatalyst was immobilised onto Polytetrafluoroethylene (PTFE) fibres.

***Keywords*:** TiO_2, CO_2 reduction, photocatalysis, formic acid

1. Introduction

Photocatalytic CO_2 reduction converts CO_2 to other chemicals using light as the energy input.[1] Titanium dioxide (TiO_2) has been regularly used for Ultraviolet (UV) induced photocatalysis due to its abundance, low cost, and having sufficient positive and negative redox potentials in the conduction band and valence band. TiO_2 in its anatase form is the most suitable for photocatalytic reactions due to its larger surface area, stability and higher activity compared to its rutile or brookite form.[2]

The idea of direct photocatalytic CO_2 reduction in rich amine is in line with the concept of Integrated Carbon Capture and Utilization (ICCU). Rich amine is the amine stream that leaves the CO_2 absorption tower and is loaded with CO_2, to be regenerated and recycled back into the system. The concept of ICCU involves direct CO_2 desorption and conversion from the rich amine. This removes the need for a CO_2 purification process, compression, and transportation, and would significantly improve energy efficiency.[3] Among various products that can be synthesized from CO_2, methanol and formic acid are of high interest for the ICCU.[4] Tai et al. reported a methanol yield of 31.49 μmol/gcat.h from direct photocatalytic CO_2 reduction using Mg-TiO_2 in rich amine.[5]

DOI: https://doi.org/10.37256/sce.7120268643

Attractively, producing formic acid requires only two electron transfers, $CO_2 + 2H^+ + 2e^- \rightarrow HCOOH$, whereas reduction to methanol requires six.[6,7] Formic acid is a carboxylic acid with a wide range of applications, one that is gaining attention is its use as an energy carrier (4.4 wt% H_2 in formic acid).[4] The industry standard requires most formic acid to be in a concentration of 85%, with its use as a chemical intermediate to manufacture chemicals and pharmaceuticals and as a preservation/ animal feed additive.[8]

Since amine solutions are basic, the photocatalytic system in basic conditions is expected to follow a parallel reaction scheme as shown in Figure 1 as theorized by Galli et al.[9] In addition to the consecutive path, formaldehyde would form autonomously from formic acid. Gas phase products (CO and H_2) will also form consecutively through photoreforming of the formaldehyde and formic acid. Hence, to target formic acid production, the process reaction has to be carried out at an optimum condition, otherwise its concentration would decrease as it could be converted to other chemicals.

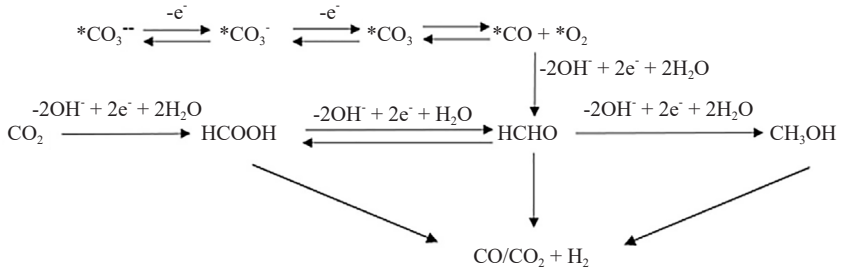

Figure 1. Parallel reaction scheme for molecular CO_2 and carbonate photoreduction produced by Galli et al.[9]

When CO_2 is absorbed by a tertiary amine solution such as Methyldiethanolamine (MDEA), it reacts chemically with the amine and becomes bicarbonate. Pan et al.[10] described that bicarbonate (HCO_3^-) can be reduced by electrons to form formate, but it can also be oxidized to carbonate by holes or hydroxyl radicals. In a mechanistic study by Nguyuen et al.,[11] the photocatalytic HCO_3^- reduction could lead to the formation of formate, methanol, and acetate.

To find the optimum condition for the photocatalytic process, Response Surface Methodology (RSM) can be employed to optimize many process parameters whilst reducing the number of experiments. This method can simultaneously evaluate the effects of several process variables and determine the impact of each independent variable and its combined effect.[12,13] The RSM concept has been used and reported by some researchers in photocatalysis CO_2 conversion, with the Central Composite Design (CCD) being the most used. For example, Chakrabortty et al.,[14] used CCD to reach the optimum condition for the photoconversion of CO_2 to methanol. Delavari et al.,[13] used a central composite rotatable design to evaluate photocatalytic conversion of immobilized TiO_2 coated on a mesh, and Firoozabadi et al.[15] applied a face-centered composite design to study the effect of temperature, UV light power, and partial pressures of CO_2 and H_2O on its reaction. Apart from that, the Box-Behnken Design (BBD) is also another widely preferred design for RSM, especially in photocatalytic degradation.[16-18] It required three levels for each factor, hence fewer experimental runs and is used to fit a second-order model.[17] This study looks at optimizing photocatalytic temperature, reaction duration and the amount of photocatalyst used.

To understand the kinetics of heterogeneous catalytic processes, Langmuir-Hinshelwood (LH) kinetics is the most commonly used kinetic expression.[19] LH kinetic models reported for CO_2 photoreduction involve diffusion and adsorption of CO_2 onto the surface of the photocatalyst, generation of electron-hole pairs and photoreaction, and finally the desorption of products from the surface.[20] Understanding the kinetics of CO_2 photoreduction to produce formic acid using TiO_2 is important for practical process scale-up in the future. Kinetic constants and good model fit are determined based on proposed models in the literature.[21]

In further consideration of pursuing ICCU, slurry photocatalytic systems are commonly used, but immobilised photocatalysts would help to prevent them from being easily washed away.[22] In our previous study, TiO_2 had been successfully immobilised onto Polytetrafluoroethylene (PTFE) membrane surfaces.[23] Immobilizing photocatalysts onto solid supports has emerged as a practical strategy to improve catalyst stability, facilitate recovery, and enable continuous

operation in photocatalytic systems. Thus, a comparison between slurry and immobilised photocatalyst systems is important in developing the technology.

This study aims to optimize the photocatalytic reduction of CO_2 in rich amine to formic acid using TiO_2 through the response surface methodology. It further seeks to model the reaction kinetics to better understand the governing mechanisms. Additionally, the performance of slurry TiO_2 is compared with that of immobilized TiO_2 to evaluate their suitability for integrated carbon capture and utilization applications.

2. Experimental methodology

2.1 *Materials*

Titanium (IV) oxide (TiO_2) anatase (99.7% trace metal basis) was purchased from Sigma Aldrich. Properties of the TiO_2 are listed in Table 1 below. For photocatalytic CO_2 reduction performance testing, N-Methyl-2,2'-iminodiethanol (MDEA) and piperazine anhydrous were used as the medium and were purchased from Merck.

For TiO_2 immobilization, Polytetrafluoroethylene (PTFE) hollow fibre membranes were produced and supplied by Dalian Institute of Chemical Physics (DICP). All materials were used without further purification.

Table 1. Properties of the photocatalyst TiO_2 anatase

TiO_2 particle characteristics	Value
BET surface area (m^2/g)	96.7
Pore volume (cm^3/g)	0.25
Average pore size (Å)	89.1
Band-gap energy (eV)	2.91

2.2 *Analytic quantification by HPLC analysis*

To measure the amount of formic acid in the product sample, an Agilent High-Performance Liquid Chromatography (HPLC) 1,200 series system was used with a Phenomenex Rezex Organic Acid (ROA) H^+ (8%) 300 × 7.8 mm column. The analysis method is as described in Table 2.

Table 2. HPLC analysis method

Parameters	Condition
Injection volume	20 µL
Mobile phase	0.0025 mol/L H_2SO_4
Flow	0.6 ml/min
Temperature	40 °C
Detector	MWD (UV), 210 nm 16 bandwidth
Analysis time	35 min
Retention time	16.501 min (Formic acid)

The calibration curve for formic acid has a strong linear relationship between peak area and concentration across the tested range (0-50 ppm). The plotted data points fall closely along the regression line, yielding an excellent correlation coefficient of 0.99993. The low residual standard deviation (5.7176) confirms the precision and reliability of the calibration for quantitative analyses.

2.3 *Batch photocatalytic CO_2 reduction setup*

A glass reactor with a capacity of 300 ml (with a diameter of 5 cm and height of 15.3 cm) was used. The batch photoreactor setup was lit up internally using a SOBO UVC-9W double lamp (4.44-6.19 eV, 250 nm and an intensity of 2.7 mW/cm^2), similar to the previous experimental setup reported.[23,24] A magnetic stirrer was used to improve the flow of material and heat within the reactor. An oil bath was used to maintain a constant temperature, and the photoreactor setup was placed in a stainless-steel vessel which reflected light for better efficiency in light energy utilization.

The reaction medium was prepared using 45 wt% of MDEA with piperazine in a distilled water solution and bubbled directly with CO_2 to produce a CO_2-rich amine solution. The CO_2 loading of the rich amine was analysed through a titration method[25] to ensure saturation and consistency of the amount of CO_2 in the amine for every batch run, i.e., 0.5 mol CO_2/mol amine (10 wt%). Three hundred milliliters of the solution was filled into the gas-tight reactor. TiO_2 was measured and put into the medium in the photoreactor with continuous stirring, as shown in Figure 2.

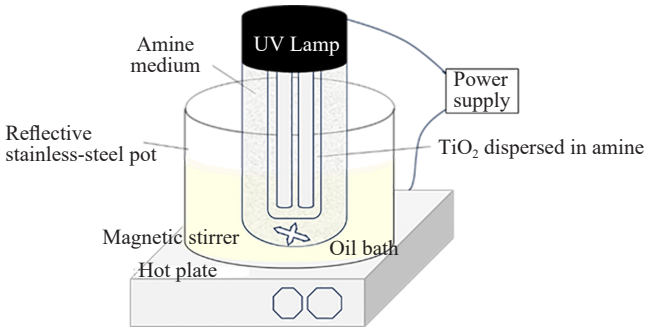

Figure 2. Schematic diagram of the batch reactor setup for photocatalytic CO_2 reduction with slurry TiO_2 dispersed in the rich amine solution

At the end of the batch reaction, liquid samples were taken and analyzed by HPLC to determine the amount of formic acid produced from CO_2 reduction. Product yield was calculated based on the analyser result, the amount of catalyst, and reaction time, as shown in Equation (1):[24]

$$\text{Product yield } (\mu\text{mol/g}\cdot\text{h}) = \frac{\text{Concentration of product } (\mu\text{mol})}{\text{catalyst amount } (\text{g}) \times \text{ reaction time } (\text{h})}. \quad (1)$$

2.4 *Experimental design using RSM method*

Table 3. Experimental factors with the set low and high levels

Factor	Name	Unit	Low level	High level	Mean
A	Time	Hour	1	3	2
B	Temperature	℃	30	50	40
C	Catalyst amount	g	0.2	1.0	0.6

The Design of Experiments (DOE) was based on a Box-Behnken design which explores the factor space without extreme corner points. The basis for low and high levels for time, reaction temperature, and catalyst amount for the experiments is described in Table 3 and is built upon the reported outcomes from previous researchers.[9,26] Fifteen experimental runs were planned for the DOE with replications of the middle point; the list of experimental conditions is tabled out in Table 4.

Table 4. Experimental design using box-behnken design for photocatalytic CO_2 reduction

No.	Reaction time (hour)	Temperature (°C)	Catalyst amount (g)
1	2	40	0.6
2	1	30	0.6
3	3	30	0..6
4	2	30	0.2
5	2	30	1.0
6	2	40	0.6
7	1	40	0.2
8	3	40	0.2
9	1	40	1.0
10	3	40	1.0
11	2	40	0.6
12	1	50	0.6
13	3	50	0.6
14	2	50	0.2
15	2	50	1.0

2.5 *Kinetic model fitting*

The optimum condition obtained from the DOE study was used for the kinetic model fitting study. The reaction was carried out up to 10 hours, with sampling carried out intermittently. The samples were analysed using HPLC as per the method mentioned above. The experimental kinetic data, which is the concentration of formic acid against time, was evaluated using a non-linear regression method.

The mathematical expression describing the reaction rate follows the Langmuir Hinshelwood model. Three models were evaluated to estimate the unknown kinetic constants. This approach is similar to that done by other researchers in selecting kinetic models that best fit the experimental data.[27] Model I is based on the model established by Astuti et. al.[28] for CO_2 photoreduction to formic acid. Model II and III are based on the model developed for methanol yield by Abdullah et al.[21] but adopted for formic acid based on the assumption that methanol produced would be from having formic acid as intermediate.[9]

Model I:

$$t = \frac{(C_{HCOOH})^2}{2k}.$$

Model II:

$$t = \frac{(C_{HCOOH})^3}{3k_1}.$$

Model III:

$$t = k_3 \lg\left(1 - k_4 \left(C_{HCOOH}\right)^{3/2}\right) + k_5 \left(C_{HCOOH}\right)^{3/2}, \text{ where } k_3 = \frac{-2k_1}{3k_2^2},\ k_4 = \frac{k_2}{k_1},\ k_5 = \frac{-2}{3k_2}.$$

PolymathPlus software was used for kinetic model fitting through a non-linear regression curve fit. The initial guess value is keyed in, and a few iterations are done to obtain the best fit. The accuracy of the kinetic model is assessed through R^2 and Root Mean Squared Deviation (RMSD).[29,30] R^2 is calculated based on the sum of squares as described in Equation (2) below. Hence, the higher the R^2 value, the better the model fits the experimental dataset. RMSD is a measure of the differences between true and predicted values, calculated by Equation (3), where the lower the RMSD, the more accurate the experimental results are relative to theoretical predictions.

$$R^2 = 1 - \frac{\sum_{j=1}^{n}\left(y_j - \hat{y}_j\right)^2}{\sum_{j=1}^{n}\left(y_j - \bar{y}_j\right)^2} \tag{2}$$

$$RMSD = \frac{1}{n}\sqrt{\sum_{j=1}^{n}\left(y_j - \hat{y}_j\right)^2} \tag{3}$$

where $\hat{y}$ is predicted or fitted value, $\bar{y}$ is mean value and n is the number of observations.

2.6 *Immobilisation of TiO_2 onto polymeric membrane surface*

TiO_2 photocatalysts were immobilised onto a PTFE membrane. The immobilisation method is described in detail in our previous paper.[23] The PTFE membrane first needs to go through a defluorination and surface grafting process, prior to the immobilisation of TiO_2 onto the surface.

Field Emission Scanning Electron Microscope with Energy Dispersive X-Ray (FESEM-EDX) (Hitachi, Model SU7000) was used to confirm the presence of silane with TiO_2, and later its presence on the polymer surface. Sample preparation involved sputtering it with platinum using Quorum Q150RS. The amount of TiO_2 immobilised on the PTFE surface was quantified by Thermogravimetric Analysis (TGA) (Mettler Toledo), based on the mass of the residue.[31,32] TGA was operated by heating from 25 °C to 800 °C at a rate of 10 °C/min with nitrogen flowing at 50 ml/min.

2.7 *Evaluation of immobilized TiO_2 on formic acid yield*

2 strands of PTFE-TiO_2 hollow fiber membrane (each of 2 m length) were placed into the photoreactor by winding around the UVC light source. The photocatalytic reaction setup is similar to that described in Section 2.3, as shown in Figure 2. In addition, for reusability testing, the PTFE-TiO_2 was used directly in the following cycles without any additional treatment. The recyclability test was conducted over 3 runs.

3. Results and discussions

3.1 *Rich amine as photocatalytic reaction medium*

Blank control tests were performed to gauge the influence of a CO_2-rich amine solution in photocatalysis and to improve confidence in the photocatalytic activity. Table 5 shows the results at varying control runs, i.e. fresh amine exposed to UV light, rich amine with TiO_2 added in, and rich amine exposed to UV light. The control runs were conducted in the same setup as shown in Section 2.3 and were run for 3 hours.

Blank control experiments showed only trace formation of formic acid (0.100-0.154 ppm) under all non-catalytic conditions, indicating minor background contributions from the rich amine matrix and UVC irradiation. Thus, this establishes that true photocatalytic production in this study must exceed ~0.15 ppm. These findings verify that the formic acid measured under optimized conditions is attributable to genuine photocatalytic activity rather than artefacts from the reaction medium or illumination.

Table 5. Blank contol test for rich amine as photocatalytic reaction medium

Sample	Bubbled with CO_2	TiO_2 added in	UV exposure	Formic acid detected (ppm)
Blank 1			×	0.100
Blank 2	×	×		0.115
Blank 3	×		×	0.154

The trace amount of formic acid detected in the sample is assumed to be due to the degradation product of the amine itself. Formic acid is one of the oxidative degradation products of MDEA and piperazine.[33] The use of amine solutions as a medium for the photocatalysis reaction is limited in literature. They have however been incorporated as electron donors and sacrificial agents (such as Triethylamine (TEA) and Triethanolamine (TEOA)) to enhance charge separation and overall photocatalytic efficiency.[34] It is interesting to note that one of the oxidative degradation products of MDEA also includes TEOA.[33] Thus, it could indirectly assist in the photocatalytic reaction. There is no reported literature however on the use of MDEA or piperazine as a hole scavenger.

3.2 *Response surface analysis*

3.2.1 *Statistical analysis*

This study looks at formic acid as the targeted product of CO_2 reduction in rich amine. The experimental runs (refer to Table 4) were carried out, and samples were analyzed through HPLC. The data were analyzed using Analysis of Variance (ANOVA) through Design-Expert software by Stat-Ease, Inc. (version 23.1.0), and the data was fitted to the best model. The resultant model has *P*-value of 0.0378 (i.e. less than 0.0500) which indicates model terms are significant, as shown in Table 6 below.

Model terms A, B, BC, and A^2 are found to be significant for the yield of formic acid. Based on the ANOVA results, factors with *p*-values less than 0.05 are considered statistically significant, indicating that they have a measurable influence on the response variable. These factors are therefore important in the response surface modeling and optimization process to ensure accurate prediction and control of the system behavior.

The model has an *F*-value of 5.48 which implies the model is significant and that there is only a 3.78% chance that it could occur due to noise. Based on the model statistics, the model has a good R^2 value of 0.9080. The model also has an adequate precision of 7.609 (i.e. a value > 4) which indicates an adequate signal and that it can effectively navigate the design space. Collectively, these statistical indicators confirm the robustness and predictive capability of the developed empirical model for optimizing the photocatalytic CO_2 reduction process. The produced empirical model is a polynomial expression that consists of 15 coefficients as follow:

Yield of formic acid (ppm) = $-5.23501 - 1.90079A + 0.291209B + 6.12328C + 0.007412AB + 0.197812AC - 0.134737BC + 0.496450A^2 - 0.002594B^2 - 1.29391C^2$.

Table 6. ANOVA result for yield of formic acid

Source	Sum of squares	df	Mean square	*F*-value	*p*-value	
Model	5.12	9	0.5684	5.48	0.0378	significant
A-Time	1.13	1	1.13	10.92	0.0214	
B-Temperature	1.06	1	1.06	10.23	0.0240	
C-Catalyst amount	0.0036	1	0.0036	0.0347	0.8596	
AB	0.0220	1	0.0220	0.2120	0.6645	
AC	0.0250	1	0.0250	0.2415	0.6439	
BC	1.16	1	1.16	11.21	0.0204	
A^2	0.9100	1	0.9100	8.78	0.0314	
B^2	0.2485	1	0.2485	2.40	0.1823	
C^2	0.1582	1	0.1582	1.53	0.2715	
Residual	0.5184	5	0.1037			
Lack of fit	0.3355	3	0.1118	1.22	0.4794	not significant
Pure error	0.1829	2	0.0915			
Cor total	5.63	14				

Table 7. Experimental result with predicted results comparison

Run	Time (hr)	Temp (°C)	Catalyst (g)	Formic acid (ppm)	
				Actual	Predicted
1	2	40	0.6	1.524	1.252
2	1	30	0.6	0.848	0.886
3	3	30	0.6	1.661	1.738
4	2	30	0.2	0.492	0.239
5	2	30	1.0	0.841	0.978
6	2	40	0.6	0.926	1.252
7	1	40	0.2	1.074	1.290
8	3	40	0.2	1.956	2.132
9	1	40	1.0	0.968	0.793
10	3	40	1.0	2.166	1.951
11	2	40	0.6	1.305	1.252
12	1	50	0.6	1.168	1.091
13	3	50	0.6	2.278	2.240
14	2	50	0.2	1.807	1.671
15	2	50	1.0	0.048	0.254

The statistical analysis of the model provides insight into the relative importance of the process parameters for photocatalytic CO_2 reduction to formic acid. Based on the ANOVA results and regression coefficients, the factors can be ranked in terms of their influence on the response as follows: reaction time > temperature > catalyst amount. This ranking suggests that the duration of the reaction plays the most critical role in determining the formic acid yield.

Within the studied time range (i.e. 1 to 3 hours), it was observed that shorter durations were insufficient to achieve the optimal formic acid yield. This suggests that the photocatalytic reduction of CO_2 requires a minimum threshold of reaction time to allow for adequate photon absorption, charge carrier generation, and subsequent surface reactions leading to the product formation. Thus, extending the reaction time closer to the upper limit of the studied range appears necessary to drive the reaction toward higher conversion efficiency.

The factors ranking is followed by the thermal energy input, while the amount of catalyst has a comparatively lesser effect within the studied range. The model term BC is significant, and it is the interaction between temperature (B) and catalyst amount (C). Based on the produced empirical model, the term BC exhibited a significant negative effect on formic acid yield, indicating that simultaneous increases in both factors reduce the response. This suggests that high catalyst loading combined with elevated temperature is detrimental to yield. Excessive catalyst loading would result in unfavorable light scattering and limit light penetration into the solution.[35]

The experimental result from the DOE is shown in Table 7 together with the predicted values based on empirical models from RSM analysis.

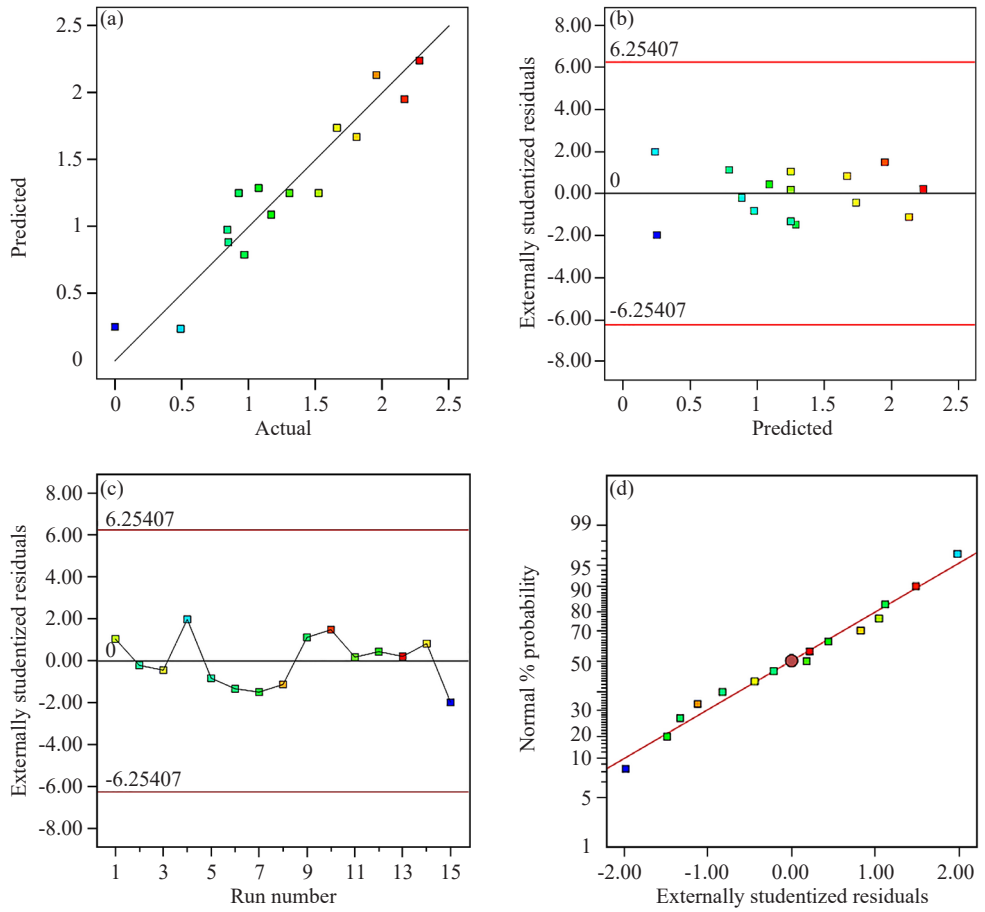

Figure 3. (a) Linear fit of predicted vs actual values, (b) Residual vs predicted diagram, (c) Residual vs run diagram, (d) Normal plot of residuals

Figure 3a presents the linear fit between predicted and actual values, demonstrating a strong correlation and indicating that the developed model is capable of accurately estimating the response variable. To further assess the

model's adequacy, residual analysis was performed. As shown in Figures 3b-c, the plots of residuals against predicted values and experimental runs reveal that all residuals fall within ± 4%. This narrow range suggests a minimal deviation between observed and predicted outcomes, reinforcing the reliability and precision of the model.[36]

The normal probability plot of the residuals shows that there are almost no violations of the basic assumptions of the analysis, which confirms the independent residuals and errors are normally distributed.[15,37] The absence of patterns or clustering in the residual plots further indicates that the model does not suffer from heteroscedasticity (observed as a funnel-shaped pattern) or autocorrelation (observed as a wave-like or cyclical pattern), thereby validating the statistical robustness of the analysis.

The developed model demonstrates a strong ability to explain the existing experimental data, as evidenced by the high coefficient of determination (R^2), low residual error, and statistically significant factors.

3.2.2 *Optimized production of formic acid and validation*

It is essential to validate the developed model's predictive capability using independent data or additional experimental runs. Validation is carried out to ensure that the model is not overfitted and can reliably generalize to new conditions beyond those used in its construction. Thus, the model is used to predict and validate the optimum condition for formic acid production.

Figure 4 shows the 3D plot illustrating the effect of reaction time and temperature on the yield of formic acid at a minimal constant catalyst amount of 0.2 g. The optimum condition to produce the highest yield of formic acid based on the model is to run the photocatalytic reaction at 50 ℃, with 0.2 g of catalyst in 300 ml solution (i.e. 0.67 g/L) for 3 hours. The model point-predicted mean of 2.662 ppm of formic acid from the reaction; whilst the validation run using the optimized condition produced 2.730 ppm of formic acid as shown in Table 8 below.

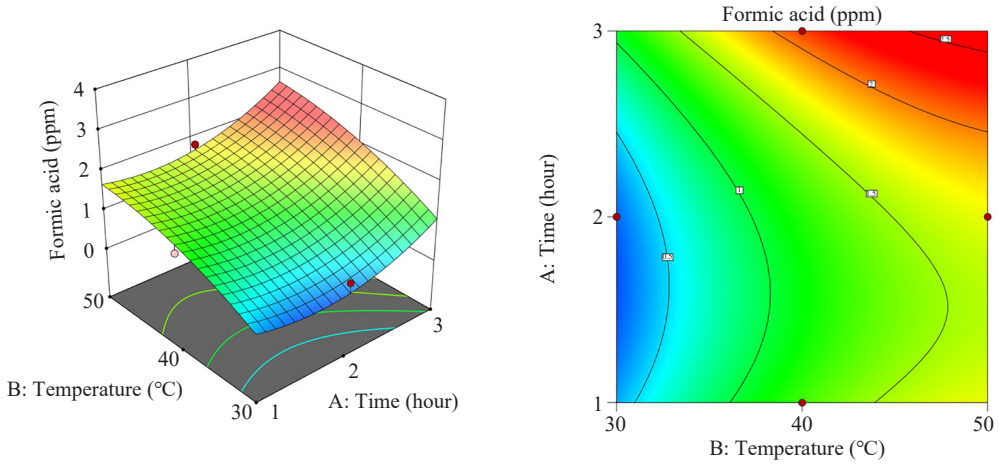

Figure 4. Interaction effect of reaction time and temperature against yield of formic acid at constant catalyst amount of 0.2 g

Table 8. Validation run of optimized condition

Run	Time (hr)	Catalyst (g)	Temp (℃)	Formic acid (ppm)		Yield (µmol/g cat·hr)	
				Actual	Predicted	Actual	Predicted
1	3	0.2	50	2.8327	2.6621	102.5655	96.3914
2	3	0.2	50	3.0048	2.6621	108.7991	96.3914
3	3	0.2	50	2.3509	2.6621	85.1218	96.3914
Average	3	0.2	50	2.7295	2.6621	98.8288	96.3914

The optimum conditions were proven to produce the highest amount of formic acid among the results evaluated in the ANOVA. Successful validation further supports the model's applicability for guiding process optimization and future scale-up efforts.

3.3 *Comparative analysis of optimized production of formic acid*

Results in Table 9 compare the formic acid yield in this study against those reported in the literature. The use of rich amine as a medium is scarce in literature, but NaOH is commonly used to tune the pH of the reaction medium to be basic. Most of the photocatalytic reactions are observed to run for longer periods of up to 8-10 hours[38,39] which is not favorable for process scale up. Longer reaction times mean less product per unit time, which reduces overall productivity. It also means higher operational expenses, making it less competitive economically.

Comparatively, Galli et al.[40] show a competitive outlook with a yield of 2,954 µmol/gcat/h after a similar 3 hours of reaction. The researchers, however, employed the addition of 2.0 g of hole scavenger (i.e. sodium sulphite, Na_2SO_3) which was completely consumed during the reaction, and operated at a higher temperature and pressure of 80 °C and 7 bar, respectively. The increased pressure likely contributed to the enhanced yield by increasing the solubility and availability of CO_2 in the reaction medium, thereby improving the mass transfer and reaction kinetics. This observation suggests that CO_2 concentration plays a critical role in determining the efficiency of formic acid production.

Table 9. Comparison against result in literature

Photocatalyst	Formic acid produced (µmol/g cat·hr)	Light source	Reaction medium	Reaction duration (hrs)	Reference
TiO_2	108.00	UVC-9 W	MDEA-PZ solution	3	This study
TiO_2	2,954.00	25 W Hg vapour lamp	Water with NaOH and Na_2SO_3	3	Galli et al.[40]
N-TiO_2/CuO	1,980.00	Xenon lamps (40 W)	Water	3	Ibarra-Rodriguez et al.[41]
TiO_2	59.80	500 W Xenon lamp	TEA solution	4	Astuti et al.[28]
TiO_2	16.38	UV-VIS lamp 300 W and Xe-Halogen lamp 400 W	Water with NaOH and H_3PO_4	8	Mele et al.[38]
TiO_2-CuPc	208.50	HRC UV-VIS lamp 300 W and Xe-Halogen lamp 400 W	Aqueous phosphoric acid solution at pH = 3	8	Mele et al.[42]
TiO_2-CuPc	65.20	HRC UV-VIS lamp 300 W and Xe-Halogen lamp 400 W	0.1 M NaOH solution	8	Mele et al.[42]
TiO_2-CuPc	26.06	UV-VIS lamp 300 W and Xe-Halogen lamp 400 W	Water with NaOH and H_3PO_4	8	Mele et al.[38]
TiO_2	22.10	500 W tungsten-halogen lamp	NaOH aqueous solution	10	Zhao et al.[39]
TiO_2-CoPc	148.76	500 W tungsten-halogen lamp	NaOH aqueous solution	10	Zhao et al.[39]
TiO_2	0.27	990 W Xenon lamp	Purified water	30	Kaneco et al.[43]

Ibarra-Rodriguez et al.[41] have also reported a high yield of formic acid at 3 hours of reaction with 1,980.00 µmol/gcat/h. Whilst their reaction conditions (i.e. 50 °C and 0.13 bar) are close to the ones used in this study, they carried out an extensive study to modify the TiO_2 catalyst. The TiO_2 was impregnated with CuO and nitrogen-doped to achieve higher affinity for adsorbing CO_2 molecules and its high electronegativity increased CO_2 reactivity and conversion.

It is interesting to observe that in one of the studies, Mele et al.[42] have used an acidic medium instead of the common basic medium approach. They achieved a fair yield of formic acid of 208.5 µmol/gcat/h after 8 hours of reaction. The researchers reported from their observation that the conversion of CO_2 into formic acid increased by decreasing the pH value in their set of experiments. This was because acidic pH favors the desorption of formic acid from the photocatalyst surface. Perhaps future research could delve further into the impact of low pH on facilitating

desorption from the photocatalyst surface.

In summary, the formic acid yield obtained in this study is considered promising, particularly given the simplicity of the system employed. The photocatalytic reaction was conducted under ambient conditions without the use of elevated pressure or temperature, which enhances the practicality and scalability of the process. Furthermore, no hole scavenger was introduced, and the TiO_2 photocatalyst was used without any extensive surface modification. These factors demonstrate the inherent effectiveness of the system and suggest that further enhancements could be achieved through targeted catalyst engineering.

3.4 *Kinetic model fitting*

CO_2 photoreduction reaction was carried out over 10 hours and sampled periodically. The production of formic acid (μmol/g cat) over time is as shown in Figure 5 below. The model fitting is limited to the production of formic acid (i.e. the first 3 hours of reaction) and does not describe how over time the formic acid would eventually be photodegraded and consumed or formed into other products, such as formaldehyde and methanol.[9] This observation is similar to the trend reported by Galli et al.,[28] where, when the duration of the reaction is prolonged, formic acid would eventually be photodegraded and consumed, and gas phase products such as CO and H_2 were detected after prolonged reactions and would steadily increase with reaction time. Thus, the kinetic model fitting in this study focus on the formation of formic acid in the first 3 hours of the reaction.

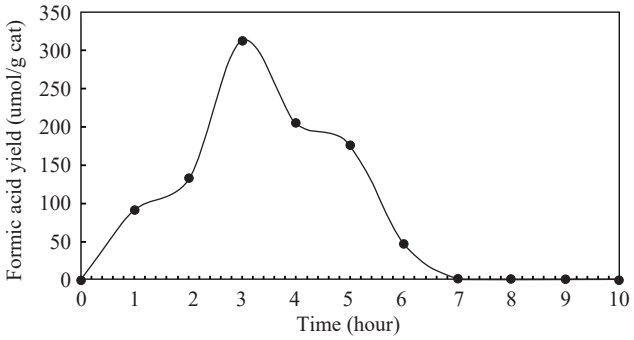

Figure 5. Production of formic acid (μmol/g cat) over time

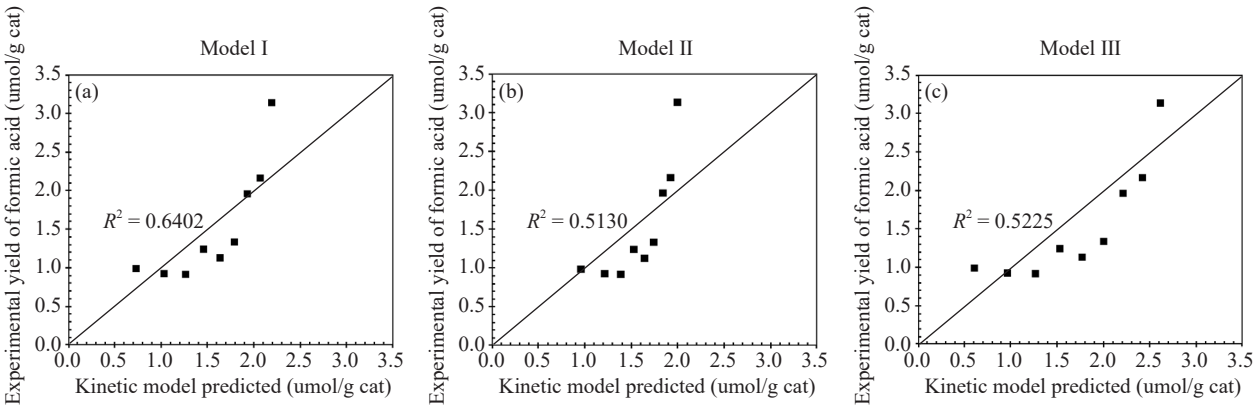

Figure 6. Comparison of the experimental rate with kinetic model predicted rate for (a) Model I, (b) Model II and (c) Model III

Three kinetic models are evaluated and used to fit experimental data. Model I is based on the model established by Astuti et al.[42] for CO_2 photoreduction to formic acid. Model II and Model III are based on models developed for methanol yield by Abdullah et al.[21] but adopted for formic acid based on the assumption that methanol produced would

be from having formic acid as an intermediate.[40]

The result of the model data fitting can be observed in Figures 6 and 7, and Table 10. The R^2 obtained is within the range of 0.50-0.65, indicating a moderate level of correlation between the predicted and actual values.

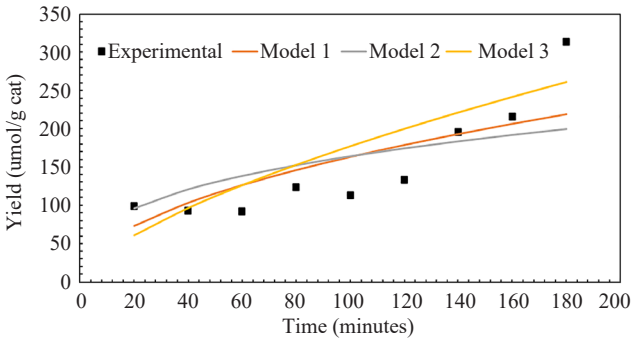

Figure 7. Comparison of the experimental data with fitted kinetic model over the 3-hour reaction time

Table 10. Result of kinetic data for slurry system by non-linear regression

Equation	Ref.	Constant	R^2	RMSD	Variance	95% confidence
Model I	Astuti et al.[28]	k = 7,996.9826	0.6402	14.0896	3,375.84	2,009.98
Model II	Abdullah et al.[21]	k_1 = 885,531.8	0.5130	16.3936	660,292	2,721.10
Model III	Abdullah et al.[21]	k_3 = -7,307.74 k_4 = -1.015E-05 k_5 = 0.0742	0.5225	11.8941	1,432.37	2.4825

Model I is based on the simplified rate expression $t = \frac{(C_{HCOOH})^2}{2k}$, assuming a second-order dependence on formic acid concentration. This model yielded a rate constant k = 7,996.98 μmol^2/(L·gcat)^2·h. The model showed a moderate fit with a R^2 value of 0.6402 and RMSD of 14.09. Model I is the best fit amongst the several models evaluated representing the data on photocatalytic CO_2 reduction to formic acid. Model II is a more complex expression incorporating higher-order terms, resulting in a rate constant k = 885,531.8 μmol^3/(L·gcat)^3·h. Despite its complexity, the model had a lower R^2 of 0.5130 and higher RMSD of 16.39, indicating poorer fit compared to Model I. Model III is a polynomial-based model with multiple constants and had the lowest RMSD (11.89), and the R^2 of 0.5225 suggests limited predictive reliability.

Astuti et al.[44] described that Model I is based on the assumption that only one reactant (CO_2 or H_2O) undergoes chemisorption on the catalyst surface, while the other reacts via physisorption. Model II by H Abdullah et al.,[21] in contrast is based on assumption that two reactants (CO_2 and H_2O) are chemisorbed onto the catalyst surface. The schematic description is as shown in Figure 8. Hence, it can be roughly deduced that only one reactant undergoes chemisorption on the catalyst surface.

Comparing the kinetic constant obtained from Model I (i.e. k = 0.007997 mol^2/(L·gcat)^2·h. Against the literature, it is encouraging that it is found to be comparable to the values reported by Astuti et al.,[45] in their work with ZnO-ZnS heterojunction photocatalysts on CO_2 reduction to formic acid. They reported their kinetic constant to be in the range of 0.002-0.012 mol^2/(L·gcat)^2·h whilst varying the photocatatlyst composition and calcination temperature.

Although Model I demonstrated the best fit among the three kinetic models evaluated, its coefficient of determination (R^2 = 0.6402) indicates only a moderate correlation between the predicted and experimental data. One plausible explanation for this is the preloaded rich amine condition used in this study. The rich amine was introduced to simulate the downstream photocatalytic conversion of CO_2 that had already been captured in a prior absorption step, thereby mimicking conditions in an integrated CO_2 capture and utilization (ICCU) system.

In contrast, many studies in the literature employ a continuous flow of gaseous CO_2 directly into the photocatalytic reactor.[21] In continuous flow systems, CO_2 interacts directly with the catalyst surface, allowing kinetic models to more accurately represent the adsorption and conversion dynamics of molecular CO_2. Whereas, in the present study, CO_2 is predominantly present in absorbed forms, such as carbonate or bicarbonate species, bound within the amine matrix. These species may exhibit different reaction pathways, rates, and accessibility to the catalyst surface compared to free CO_2 gas. As a result, the kinetic model may not fully capture the complexities introduced by the amine-mediated CO_2 delivery, leading to a lower R^2 value.

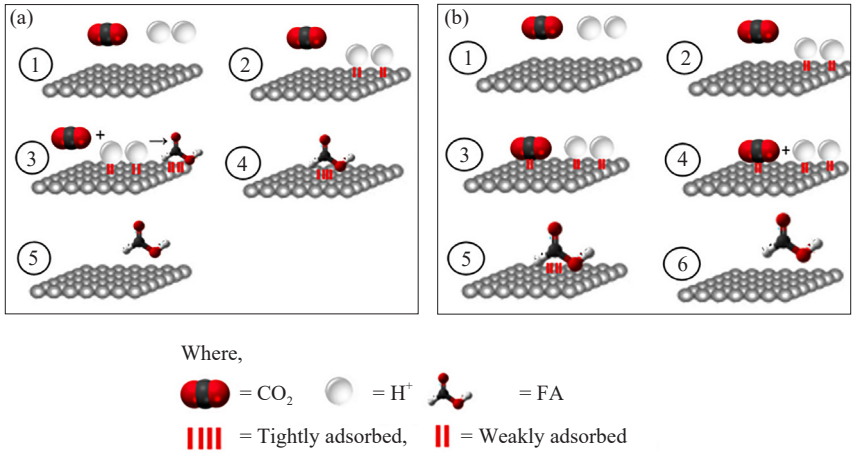

Figure 8. Possible schematic adsorption structures of CO_2, $2H^+$, and HCOOH for (a) Model I and (b) Model II[45]

This suggests that while Model I is moderately appropriate, its predictive accuracy is inherently limited by the feed chemistry and reaction mechanism. Future model development could consider how carbonate or bicarbonate species might be incorporated for CO_2 photoreduction.

3.5 *Performance of immobilised TiO_2 for CO_2*

3.5.1 *Immobilisation of TiO_2 onto polymeric membrane surface*

The amount of TiO_2 immobilized onto the PTFE is quantified based on the residue after decomposition of the polymer in TGA. Upon analysis, TiO_2 immobilised onto PTFE is 11.32 wt%. Comparing this against literature, Dekkouche et al. reported TiO_2 immobilisation of 11.0 wt%, 2.7 wt% and 3.3 wt% on their Polysulfone (PS), PTFE and Polyvinylidene Fluoride (PVDF) membranes, respectively.[31] Hence, considerably good amounts of TiO_2 are immobilized on the membrane.

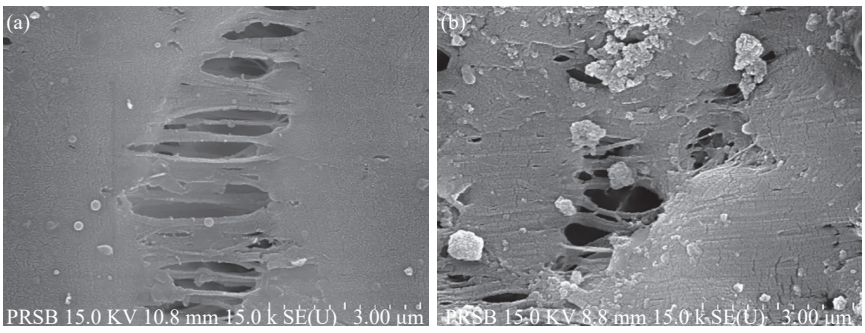

Figure 9. FESEM EDX of (a) neat PTFE membrane and (b) PTFE-TiO_2

Figure 9 shows an FESEM image of the PTFE surface with the immobilized TiO_2. No major changes took place in terms of the hollow fibre membrane diameter and thickness after the process. Leaching tests were carried out for the immobilized PTFE as shown in Figure 10. The amount of TiO_2 was found to be reduced and leached out over time.

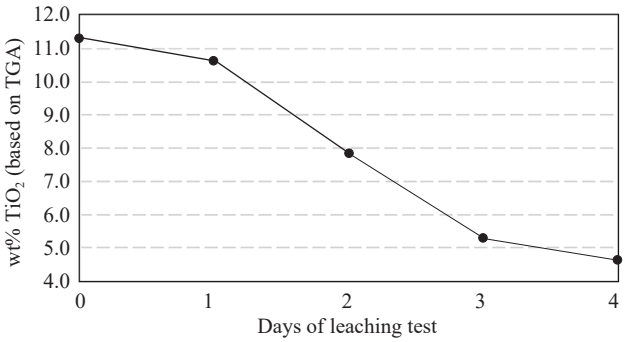

Figure 10. Leaching test result of PTFE-TiO_2 after 4 days

3.5.2 *Testing of optimised condition with immobilised TiO_2*

TiO_2 immobilised onto the PTFE membrane is tested for formic acid under the same optimised condition (i.e. 50 °C and 3 hours of reaction). The immobilised photocatalyst system produced 73.07 µmol/g cat·hr of formic acid, as shown in Figure 11. This is about a 33% drop in performance from the slurry system.

It can be deduced that this is due to limited access to direct light exposure for the photocatalysts available in the reaction. Similar observations were made by other researchers when studying immobilised photocatalysts; Espindola et al.[46] reported that the efficiency of oxytetracycline removal was higher when using TiO_2-P25 slurry due to the higher photocatalyst surface area, and Gowland et al.[47] described that the suspended catalyst outperformed the immobilised catalyst reactions, achieving a 99% reduction in the Natural Organic Matter (NOM) concentration when compared to an 89% reduction. Encouragingly, the yield of formic acid produced (i.e., 73.07 µmol/g cat·hr) is still considerably comparable with that reported in the literature (as compared in Table 6).

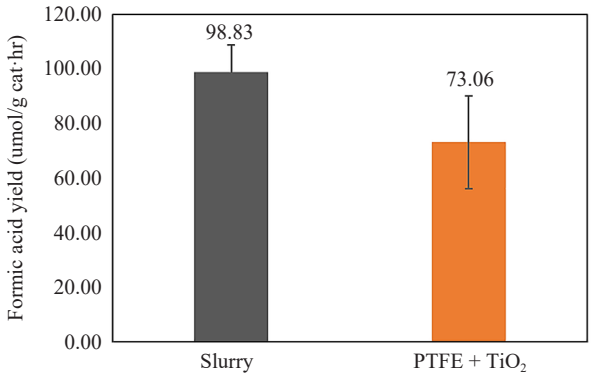

Figure 11. Comparison between slurry against immobilized TiO_2 system for photocatalytic CO_2 reduction to formic acid

3.5.3 *Reusability evaluation of the immobilized PTFE-TiO_2*

Following the evaluation of photocatalytic performance, it is equally important to assess the reusability and stability of the immobilised PTFE-TiO_2 catalyst over multiple cycles. Reusability is a key factor in determining the practical viability of immobilised photocatalysts, especially for continuous or long-term applications.

The performance of the catalyst across repeated usage cycles is examined, with particular attention to yield reduction. It is observed that the yield for immobilized PTFE + TiO_2 drops by about 18-23% after each cycle (i.e. from 73 µmol/g cat·hr to 46 µmol/g cat·hr by the third cycle) as shown in Figure 12. The drop in performance is likely due to some amount of the photocatalysts leaching out over time after use. As reported, the amount of TiO_2 immobilised dropped by half after 4 days of leaching tests. Hence, less TiO_2 is available for formic acid production.

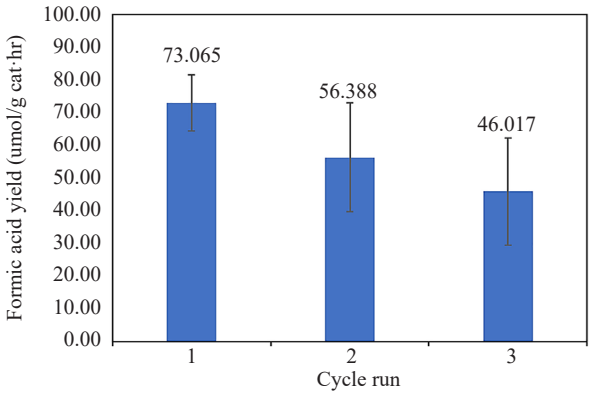

Figure 12. Recyclability testing of immobilized TiO_2 for formic acid production

3.6 *Future application of rich amine for photocatalytic CO_2 reduction*

The findings of this study demonstrate that direct photocatalytic CO_2 reduction in rich amine is feasible, with formic acid successfully generated under UVC-irradiated TiO_2 slurry conditions. However, the required reaction time of three hours and the resulting ppm-level product concentrations highlight significant process limitations. The low yield complicates the downstream separation process for obtaining the formic acid product. The long duration also prevents the treated amine from being recycled efficiently into the absorption loop, posing a major barrier to continuous ICCU operation. These challenges indicate that, in its current form, photocatalytic regeneration of the full rich-amine stream is not yet practical from a process-engineering standpoint.

To progress toward industrially viable ICCU implementation, future research should focus on strategies that intensify photocatalytic performance and reduce energy demands. From an engineering perspective, a more realistic approach may involve treating only a slip stream of the rich-amine circuit rather than the entire solvent inventory, enabling partial CO_2 conversion while maintaining stable solvent circulation. Catalyst innovation remains essential, including TiO_2 surface modification, metal/non-metal doping, and heterojunction engineering to enhance charge separation and improve reaction rates. Transitioning to visible-light-responsive catalysts would further improve process economics by reducing the reliance on high-energy UVC sources and enabling better utilization of solar or low-cost Light-Emitting Diode (LED) illumination. These directions collectively offer a pathway toward higher conversions, shorter reaction times, and more energy-efficient ICCU operation.

4. Conclusion

The photoreduction of CO_2 has been explored for formic acid production in rich amine. Optimisation was carried out through a design of experiments based on the Box-Behnken design, optimising the reaction temperature, duration, and catalyst amount. Based on response surface analysis, the optimum amount of 108 µmol/g cat·hr was achieved when running at 50 °C and 3-hour of operation, and this was comparable to literature results. The RSM empirical model has a good R^2 value of 0.9080, and was successfully validated. This optimum condition of the slurry system was then used for kinetic model fitting and comparison against immobilised photocatalysts. A moderate level of correlation for the kinetic model fit was achieved for formic acid production with R^2 of 0.64 and RMSD of 14.08. Two immobilisation methods

were attempted: one using TiO_2 directly, whilst the other used silane-functionalised TiO_2 to improve its bonding. A 33% drop in formic acid yield was observed compared to the slurry system, and subsequent running cycles observed a further drop of 18-23%.

Acknowledgment

This work was jointly produced by PETRONAS Research Sdn Bhd and Universiti Teknologi PETRONAS and funded by Petroliam Research Fund. We would like to express our gratitude for the financial support from Gastech PETRONAS (MRA Grant No. 015MD0-065).

Conflicts of interest

The authors have no competing interests to declare that are relevant to the content of this article.

References

[1] Du, C.; Wang, X.; Chen, W.; Feng, S.; Wen, J.; Wu, Y. A. CO_2 transformation to multicarbon products by photocatalysis and electrocatalysis. *Mater. Today Adv.* **2020,** *6*, 100071.

[2] Ola, O.; Maroto-valer, M. M. Review of material design and reactor engineering on TiO_2 photocatalysis for CO_2 reduction. *J. Photochem. Photobiol. C: Photochem. Rev.* **2015,** *24*, 16-42.

[3] Lv, Z.; Chen, S.; Huang, X.; Qin, C. Recent progress and perspective on integrated CO_2 capture and utilisation. *Curr. Opin. Green Sustain. Chem.* **2023,** *40*, 100771.

[4] Kar, S.; Goeppert, A.; Prakash, G. K. S. Integrated CO_2 capture and conversion to formate and methanol: Connecting two threads. *Acc. Chem. Res.* **2019,** *52*, 2892-2903.

[5] Tai, X. H.; Zain, M. M.; Saleh, S. M.; Quek, V. C.; Oh, P. C. A novel photocatalytic integrated carbon capture and utilization (ICCU) approach for conversion of CO_2 to methanol in amine solution. In *Offshore Technology Conference Asia (OTC Asia) 2024*; Kuala Lumpur, Malaysia, 2024.

[6] Pan, H.; Heagy, M. D. Photons to formate-A review on photocatalytic reduction of CO_2 to formic acid. *Nanomaterials* **2020,** *10*, 2422.

[7] Ibarra-Rodriguez, L. I.; AlfaroCruz, M. R.; Garay-Rodriguez, L. F.; Hernandez-Majalca, B. C.; Domínguez-Arvizu, J. L.; López-Ortiz, A.; Torres-Martínez, L. M.; Collins-Martínez, V. H. Photocatalytic reduction of CO_2 over Ni-Cu_xO thin films towards formic acid production. *J. Mater. Res. Technol.* **2023,** *26*, 137-149.

[8] S&P Global Formic Acid Commodity. https://www.spglobal.com/commodityinsights/en/ci/products/formic-acid-chemical-economics-handbook.html (accessed Apr. 24, 2024).

[9] Galli, F.; Compagnoni, M.; Vitali, D.; Pirola, C.; Bianchi, C. L.; Villa, A.; Prati, L.; Rossetti, I. CO_2 photoreduction at high pressure to both gas and liquid products over titanium dioxide. *Appl. Catal. B: Environ.* **2017,** *200*, 386-391.

[10] Pan, H.; Steiniger, A.; Heagy, M. D.; Chowdhury, S. Efficient production of formic acid by simultaneous photoreduction of bicarbonate and oxidation of glycerol on gold-TiO_2 composite under solar light. *J. CO_2 Util.* **2017,** *22*, 117-123.

[11] Nguyen, V. C.; Nimbalkar, D. B.; Huong, V. H.; Lee, Y. L.; Teng, H. Elucidating the mechanism of photocatalytic reduction of bicarbonate (aqueous CO_2) into formate and other organics. *J. Colloid Interface Sci.* **2023,** *649*, 918-928.

[12] Ahadzi, E.; Ramyashree, M. S.; Priya, S. S.; Sudhakar, K.; Tahir, M. CO_2 to green fuel: Photocatalytic process optimization study. *Sustain. Chem. Pharm.* **2021,** *24*, 100533.

[13] Delavari, S.; Amin, N. A. S. Photocatalytic conversion of CO_2 and CH_4 over immobilized titania nanoparticles coated on mesh: Optimization and kinetic study. *Appl. Energy* **2016,** *162*, 1171-1185.

[14] Chakraborttya, S.; Nayak, J.; Ruj, B.; Pal, P.; Kumare, R.; Banerjeea, S.; Sardarf, M.; Chakraborty, P. S. Photocatalytic conversion of CO_2 to methanol using membrane-integrated green approach: A review on capture, conversion and purification. *J. Environ. Chem. Eng.* **2020,** *8*, 103935.

[15] Firoozabadi, S. R.; Khosravi-Nikou, M. R.; Shariati, A. CO_2 photoreduction using TiO_2 nanoflower/UiO-66 composite under UV light irradiation. *J. Environ. Chem. Eng.* **2023,** *11*, 110978.
[16] Ul Hassan, S.; Shafique, S.; Palvasha, B. A.; Saeed, M. H.; Naqvi, S. A. R.; Nadeem, S.; Irfan, S.; Akhter, T.; Khan, A. L.; Nazir, M. S.; et al. Photocatalytic degradation of industrial dye using hybrid filler impregnated polysulfone membrane and optimizing the catalytic performance using Box-Behnken design. *Chemosphere* **2023,** *313*, 137418.
[17] Mohammed, N.; Palaniandy, N. P.; Shaik, F.; Mewada, H.; Balakrishnan, D. Comparative studies of RSM Box-Behnken and ANN-Anfis fuzzy statistical analysis for seawater biodegradability using TiO_2 photocatalyst. *Chemosphere* **2023,** *314*, 137665.
[18] Ali, H.; Yasir, M.; Ngwabebhoh, F. A.; Sopik, T.; Zandraa, O.; Sevcik, J.; Masar, M.; Machovsky, M.; Kuritka, I. Boosting photocatalytic degradation of estrone hormone by silica-supported g-C_3N_4/WO_3 using response surface methodology coupled with Box-Behnken design. *J. Photochem. Photobiol. A Chem.* **2023,** *441*, 114733.
[19] Kumar, K. V.; Porkodi, K.; F. Rocha, F. Langmuir-Hinshelwood kinetics-A theoretical study. *Catal. Commun.* **2008,** *9*, 82-84.
[20] Thompson, W. A.; Fernandez, E. S.; Maroto-Valer, M. M. Probability Langmuir-Hinshelwood based CO_2 photoreduction kinetic models. *Chem. Eng. J.* **2019,** *384*, 123356.
[21] Abdullah, H.; Khan, M. M. R.; Yaakob, Z.; Ismail, N. A. A kinetic model for the photocatalytic reduction of CO_2 to methanol pathways. *IOP Conf. Ser.: Mater. Sci. Eng.* **2019,** *702*, 012026.
[22] Ali, A.; Tahir, M. Recent advancements in engineering approach towards design of photo- reactors for selective photocatalytic CO_2 reduction to renewable fuels. *J. CO_2 Util.* **2018,** *29*, 205-239.
[23] Saleh, S. M.; Oh, P. C.; Zain, M. M.; Quek, V. C.; Zulkifli, A. S.; Chew, T. L. Revolutionizing CO_2 reduction with TiO_2 photocatalyst immobilized on polytetrafluoroethylene (PTFE) membrane. *J. Ind. Eng. Chem.* **2024,** *131*, 230-239.
[24] Yusop, N. M.; Oh, P. C.; Sufian, S.; Zain, M. M. Enhanced effect of metal sulfide doping (MgS-TiO_2) nanostructure catalyst on photocatalytic reduction of CO_2 to methanol. *Sustainability* **2023,** *15*, 10415.
[25] Yusop, N. M.; Norfadilah, D.; Siti Aishah, M. R.; Chan, Z. P.; Saleh, S. M. Monitoring of CO_2 absorption solvent in natural gas process using fourier transform near-infrared spectrometry. *Int. J. Anal. Chem.* **2020,** *2020*, 1-9.
[26] Qin, G.; Zhang, Y.; Ke, X.; Tong, X.; Sun, Z.; Liang, M.; Xue, S. Photocatalytic reduction of carbon dioxide to formic acid, formaldehyde, and methanol using dye-sensitized TiO_2 film. *Appl. Catal. B* **2013,** *129*, 599-605.
[27] Nascimento, I. G.; Magalhães, B. C.; Beltrame, T. B.; Segtovich, I. S. V.; Sermoud, V. M.; Zotin, J. L.; Da Silva, M. A. P. Kinetic modeling of deep simultaneous dibenzothiophene and 4,6-dimethyldibenzothiophene hydrodesulfurization over NiMoP/Al_2O_3 catalyst. *Chem. Eng. Sci.* **2024,** *288*, 119829.
[28] Astuti, A. R. A.; Saputera, W. H.; Ariono, D.; I. G. Wenten, I. G.; Sasongko, D. Membrane contactor-photocatalytic hybrid system for carbon dioxide capture and conversion to formic acid. *Results Eng.* **2024,** *22*, 102085.
[29] Tai, X. H.; Lai, C. W.; Yang, T. C. K.; Chen, C.-Y.; Abdullah, A. H.; Lee, K. M.; Juan, J. C. Effective oxygenated boron groups of boron-doped photoreduced graphene oxide for photocatalytic removal of volatile organic compounds. *J. Environ. Chem. Eng.* **2022,** *10*, 108047.
[30] Guo, L.; Harvey, J. N. Kinetic modelling of cobalt-catalyzed propene hydroformylation: A combined ab initio and experimental fitting protocol. *Catal. Sci. Technol.* **2024,** *14*, 961-972.
[31] Dekkouche, S.; Morales-Torres, S.; Ribeiro, A. R.; Faria, J. L.; Fontàs, C.; Kebiche-Senhadji, O.; Silva, A. M. T. In situ growth and crystallization of TiO_2 on polymeric membranes for the photocatalytic degradation of diclofenac and 17α-ethinylestradiol. *Chem. Eng. J.* **2021,** *427*, 131476.
[32] Wanag, A.; Sienkiewicz, A.; Rokicka-Konieczna, P.; Kusiak-Nejman, E.; Morawski, A. W. Influence of modification of titanium dioxide by silane coupling agents on the photocatalytic activity and stability. *J. Environ. Chem. Eng.* **2020,** *8*, 103917.
[33] Gouedard, C.; Picq, D.; Launay, F.; Carrette, P. L. Amine degradation in CO_2 capture. I. A review. *Int. J. Greenh. Gas Control* **2012,** *10*, 244-270.
[34] Liu, H.; Zhou, H.; Yang, L.; Pan, Y.; Zhao, X.; Wang, F.; Fang, R.; Li, Y. Photocatalytic CO_2 reduction coupled with biomass-based amines oxidation over double-shelled CdS nanocages. *Catal. Commun.* **2024,** *187*, 106884.
[35] Liu, G.; Hoivik, N.; Wang, K.; Jakobsen, H. Engineering TiO_2 nanomaterials for CO_2 conversion/solar fuels. *Sol. Energy Mater. Sol. Cells* **2012,** *105*, 53-69.
[36] Gadore, V.; Singh, A. K.; Mishra, S. R.; Ahmaruzzaman, M. RSM approach for process optimization of the photodegradation of congo red by a novel $NiCo_2S_4$/chitosan photocatalyst. *Sci. Rep.* **2024,** *14*, 1118.

[37] Song, C.; Li, X.; Wang, L.; Shi, W. Fabrication, characterization and response surface method (RSM) optimization for tetracycline photodegration by $Bi_{3.84}W_{0.16}O_{6.24}$-graphene oxide (BWO-GO). *Sci. Rep.* **2016,** *6*, 37466.
[38] Mele, G.; Annese, C.; De Riccardis, A.; Fusco, C.; Palmisano, L.; Vasapollo, G.; D'Accolti, L. Turning lipophilic phthalocyanines/TiO_2 composites into efficient photocatalysts for the conversion of CO_2 into formic acid under UV-vis light irradiation. *Appl. Catal. A: Gen.* **2014,** *5*, 169-172.
[39] Zhao, Z.; Fan, J.; Xie, M.; Wang, Z. Photo-catalytic reduction of carbon dioxide with in-situ synthesized CoPc/TiO_2 under visible light irradiation. *J. Clean. Prod.* **2009,** *17*, 1025-1029.
[40] G Tommasi, M.; Gramegna, A.; Degerli, S. N.; Galli, F.; Rossetti, I. High-pressure CO_2 photoreduction, flame spray pyrolysis and type-II heterojunctions: A promising synergy. *Catalysts* **2025,** *15*(4), 383.
[41] Ibarra-Rodriguez, L. I.; Pantoja-Espinoza, J. C.; Luévano-Hipólito, E.; Garay-Rodríguez, L. F.; López-Ortiz, A.; Torres-Martínez, L. M.; Collins-Martínez, V. H. Formic acid and hydrogen generation from the photocatalytic reduction of CO_2 on visible light activated N-TiO_2/CeO_2/CuO composites. *J. Photochem. Photobiol.* **2022,** *11*, 100125.
[42] Mele, G.; Annese, C.; D'Accolti, L.; De Riccardis, A.; Fusco, C.; Palmisano, L.; Scarlino, A.; Vasapollo, G. Photoreduction of carbon dioxide to formic acid in aqueous suspension: A comparison between phthalocyanine/TiO_2 and porphyrin/TiO_2 catalysed processes. *Molecules* **2015,** *20*, 396-415.
[43] Kaneco, S.; Kurimoto, H.; Ohta, K.; Mizuno, T.; Saji, A. Photocatalytic reduction of CO_2 using TiO_2 powders in liquid CO_2 medium. *J. Photochem. Photobiol. A: Chem.* **1997,** *109*, 59-63.
[44] Astuti, A. R. A.; Ariono, D.; Wenten, I. G.; Sasongko, D.; Saputera, W. H.; Kurnia, K. A. Mechanistic insights into CO_2 photoreduction to formic acid using ZnO catalysts. *Chem. Eng. Res. Des.* **2025,** *218*, 664-673.
[45] Astuti, A. R. A.; Saputera, W. H.; Ariono, D.; Wenten, I. G.; Sasongko, D. Enhancing CO_2 capture and conversion to formic acid via a membrane-photocatalytic hybrid system with ZnO-ZnS heterojunction catalyst. *ACS Omega* **2025,** *10*, 5563-5573.
[46] Espíndola, J. C.; Cristóvão, R. O.; Mendes, A.; Boaventura, R. A. R. Photocatalytic membrane reactor performance towards oxytetracycline removal from synthetic and real matrices: Suspended vs immobilized TiO_2. *Chem. Eng. J.* **2019,** *378*, 122114.
[47] Gowland, D. C. A.; Robertson, N.; Chatzisymeon, E. Life cycle assessment of immobilised and slurry photocatalytic systems for removal of natural organic matter in water. *Environments* **2024,** *11*, 114.